

See discussions, stats, and author profiles for this publication at: <https://www.researchgate.net/publication/50224706>

Biomimetic Calcium Phosphate Crystal Mineralization on Electrospun Cellulose-Based Scaffolds

ARTICLE in ACS APPLIED MATERIALS & INTERFACES · FEBRUARY 2011

Impact Factor: 6.72 · DOI: 10.1021/am100972r · Source: PubMed

CITATIONS

52

READS

87

3 AUTHORS, INCLUDING:



Katia Rodriguez

Virginia Polytechnic Institute and State Univ...

10 PUBLICATIONS 109 CITATIONS

SEE PROFILE

Biomimetic Calcium Phosphate Crystal Mineralization on Electrospun Cellulose-Based Scaffolds

Katia Rodríguez,[†] Scott Rennekar,^{*,†,‡} and Paul Gatenholm^{§,⊥}

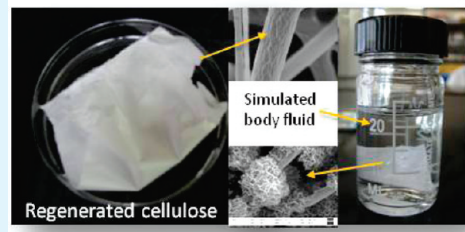
[†]Department of Materials Science and Engineering, [‡]Department of Wood Science and Forest Products, and

[§]School of Biomedical Engineering and Sciences, Virginia Tech, Blacksburg Virginia 24060, United States

[⊥]Wallenberg Wood Science Center, Department of Chemical and Biological Engineering, Chalmers University of Technology, SE41296 Goteborg, Sweden

ABSTRACT: Novel cellulose based-scaffolds were studied for their ability to nucleate bioactive calcium phosphate crystals for future bone healing applications. Cellulose-based scaffolds were produced by electrospinning cellulose acetate (CA) dissolved in a mixture of acetone/dimethylacetamide (DMAc). The resulting nonwoven CA mats containing fibrils with diameters in the range of 200 nm to 1.5 μm were saponified by NaOH/ethanol for varying times to produce regenerated cellulose scaffolds. Biomimetic crystal growth nucleated from the fiber surface was studied as a function of surface chemistry. Regenerated cellulose scaffolds of varying treatments were soaked in simulated body fluid (SBF) solution. Scaffolds that were treated with CaCl_2 , a mixture of carboxymethyl cellulose (CMC) and CaCl_2 , and NaOH and CaCl_2 , were analyzed using X-ray photoelectron spectroscopy, X-ray powder diffraction, and scanning electron microscopy to understand the growth of bioactive calcium phosphate (Ca—P) crystals as a function of surface treatment. The crystal structure of the nucleated Ca—P crystals had a diffraction pattern similar to that of hydroxyapatite, the mineralized component of bone. The study shows that the scaffold surface chemistry can be manipulated, providing numerous routes to engineer cellulosic substrates for the requirements of scaffolding.

KEYWORDS: cellulose acetate, cellulose, electrospinning, scaffold, calcium phosphate, biomimetic apatite, tissue engineering



■ INTRODUCTION

Tissue engineering is an emerging transdisciplinary field that seeks the development of scaffold materials to maintain, repair, or enhance tissue and organ function. In tissue engineering a scaffold is a support that mimics the extracellular matrix and serves as a temporary skeleton for cell growth, migration, and finally reproduction to allow tissue regeneration.¹ An ideal scaffold material for bone tissue engineering has to be biocompatible, have mechanical properties on the order of those for bone, be able to respond to specific biological signals to express and promote cell attachment, and allow for proliferation, differentiation, and finally tissue regeneration. Several studies report the applicability of cellulose-based materials for culturing cells and for implantation.^{2–5} Cellulose is the most abundant naturally occurring polymer on earth produced by plants and bacteria that has been utilized in applications from paper and textiles to materials in wound healing. Cellulose can be processed into a range of forms such as membrane sponges, microspheres, non-wovens, and knitted textiles.⁶ Strong hydrogen bonding holds together cellulose chains and accounts for the high degree of crystallinity, low solubility, and slow cellulose degradation *in vivo* for biomedical applications.^{2,7} Cellulose degradation depends on chain length, degree of crystallinity, and accessibility.^{2,4,7,8} Decreasing crystallinity and augmenting hydrophilicity of cellulose-based materials are known approaches to improve their biodegradability

in vivo.^{2,8,9} However, cellulose biodegradation has been described as a combination of mechanical, chemical, and biological processes.⁴

Biomaterials based on cellulose and its derivatives have been used as membranes for hemodialysis, carriers for immobilized enzymes, and as matrices for pharmaceuticals and drug-releasing scaffolds.^{6,10–12} Cellulose has been used in both hard and soft tissue engineering.⁶ Examples include bone regeneration,^{4,13–15} tissue engineering in postinjury brain,⁶ connective tissue formation, scaffolds for growing functional cardiac cell constructs *in vitro*,² blood vessels,^{5,16,17} artificial livers,¹⁸ expansion of progenitor hematopoietic cells in culture,¹⁹ and suppression of matrix metalloproteases action in wound healing.^{20,21} *In vitro* and *in vivo* applications of cellulose-based materials have negligible foreign body and inflammatory response reactions.^{3,4,7,22} Consequently, they are considered biocompatible.^{3,4,7} Cellulose-based material biocompatibility is further improved by functionalization with small amount of cations.^{7,8} In addition, material performance tests, such as mechanical tests, have shown cellulose stability in physiological environments after gamma sterilization and *in vitro* and *in vivo* aging.^{3,23}

Most of the biomedical application of cellulose-based materials have been used from bacterial produced cellulose,^{5,14,16,17,24–26}

Received: October 9, 2010

Accepted: February 4, 2011

Published: February 28, 2011

regenerated cellulose sponges,^{3,4} and solution spun cellulose fiber (lyocell).^{8,15,27} However, these materials do not offer the ability to control the scale of the fibers in the nano to micro diameter regions. Electrospinning is a promising technique capable of producing cellulosic fibers from a polymeric solution,²⁸ which provides the possibility to create continuous cellulose filaments of controlled diameter size for scaffold morphology design.^{10,29–33} Additionally, a key factor for a successful implantation in orthopedic applications is considered a close juxtaposition between bone and the implanted surface, which is known as osteointegration.¹³ A strategy to enhance osteointegration is surface coating the scaffold with hydroxyapatite-like minerals.^{8,26} Simulated body fluid (SBF) treatment is a usual procedure to create a surface apatite layer on biomaterials.^{8,14,26,34} SBF is an electrolyte solution that mimics the inorganic composition of the blood human plasma.⁸ Simulated body fluid (1.0 SBF) was initially designed to test the bioactivity of artificial bone material in vitro because its composition is very close to human blood plasma. SBF solutions of different concentrations (1.5 and 5 times SBF) have also been used for coating of hydroxyapatite (HA) on the surface of biointer materials with artificially introduced surface functional groups that have an ability of inducing the HA nucleation in SBF solutions.^{8,27} The formation of HA like crystals on cellulose has been successfully carried out in several studies.^{8,14,25–27} Many studies have reported that a pretreatment of the substrate with Ca²⁺ containing solution was necessary to catalyze the calcium phosphate mineralization on the scaffold during subsequent exposure to SBF solution.⁸ These studies investigated techniques to nucleate and grow calcium phosphate crystals on cellulose surfaces by modification via phosphorylation and chemical oxidation. Furthermore, functionalization with carboxyl groups in cellulose can be carried out by different means, chemically by selective oxidation reactions, exposure to plasma of oxidative gases, or physically, by adsorption of citric acid.²⁷ Irreversible adsorption of polymers containing carboxylic acid groups is another technique to enhance the number of carboxylate groups on surfaces of cellulose substrates. The irreversible adsorption of carboxymethyl cellulose (CMC) is a well described procedure in paper making.^{35,36} The attachment of CMC onto the cellulose surface is thought to be a cocrystallization process; however, the mechanism of this procedure remains conjectural.³⁶ The aim of this work was to investigate the bioactivity of electrospun regenerated cellulose scaffolds under physiological conditions and evaluate further enhancement on the biomineralization process due to CMC adsorption on the regenerated cellulose (RC) fibers.

■ EXPERIMENTAL DETAILS

Electrospinning of Cellulose Acetate. Nanofibers of cellulose acetate (CA) ($M_n = 30\,000$, 39.8% acetyl groups, Sigma Aldrich) were obtained by electrospinning method. CA powder was vacuum-dried at 50 °C and 10 mTorr prior to dissolution. Solution of CA (13%Wt/Wt) in acetone/dimethylacetamide (DMAc, 99.9%, Sigma Aldrich) (2:1) was loaded into a 10 mL disposable syringe. A syringe pump (Harvard Apparatus) was used to feed the polymeric solution at speed of 3 mL/h through a stainless steel needle with an inner diameter of 0.643 mm (Howard Electronic Instruments Inc.). A voltage of 25 kV was applied between the needle and the collector, which consisted of 10 cm × 10 cm steel mesh covered with aluminum foil. The distance between needle and collector was 25 cm. Consistencies in electrospinning CA was achieved by regulating the relative humidity in the system.

Table 1. Chemical Composition of Simulated Body Fluid Solution³⁴

order	reagent	amount (g/L)
1	NaCl	142.0
2	NaHCO ₃	103.0
3	KCl	27.0
4	Na ₂ HPO ₄ 2H ₂ O	5.0
5	MgCl ₂ 6H ₂ O	1.5
6	CaCl ₂ 2H ₂ O	2.5
7	Na ₂ SO ₄	1.0
8	(CH ₂ OH) ₃ CNH ₂	0.5

Regeneration to Cellulose. The electrospun CA scaffold was carefully removed from the aluminum foil by peeling from the edge of the mat and placed into a vacuum oven under 50 °C and 10 mTorr for 1 day. The dried CA scaffolds were immersed into 0.05 M NaOH solution in ethanol for 5, 15, 30, 45 min, or 1 day at room temperature, in order to remove acetyl group via alkali catalyzed saponification. The partially and fully regenerated cellulose scaffolds were thoroughly rinsed and kept in DI water for further treatment.

Surface Modification (CMC Adsorption). In order to generate carboxyl groups on the surface of cellulose nanofibers, the scaffolds were exposed to CMC adsorption in two ways. Procedure 1 involved exposing the scaffold to a mixture of 0.01 M CaCl₂ solution and 250 mg of CMC (100 000 g/mol, DS = 1.2) for 24 h.¹⁴ Procedure 2 consisted of exposing the scaffold to a mixture of 0.01 M CaCl₂ solution and 250 mg of CMC (100 000 g/mol, DS = 1.2) at pH 8 adjusted by addition of 0.1 N NaOH, at 80 °C for 2 h.³⁰ Subsequently, the scaffolds were treated with 0.1 M CaCl₂ solution for 24 h at room temperature for both procedures. The modified scaffolds were then placed into excess deionized water for 1 h and agitated every 15 min in order to rinse the material from ions like chlorine.

Dye Adsorption Treatment. The cellulose fibers treated with CMC were suspended in a 0.1% toluidine blue solution (20 mL/0.01 g of sample). The suspension was agitated at room temperature for 3 h, the stained fibers were washed thoroughly with ethanol (300 mL) and then water (50 mL) by filtration.³⁷ The original (control) and CMC treated electrospun fibers were observed by optical microscope (Nikon Instruments).

Conductometric Titration. The amount of charge introduced by CMC adsorption process was determined by conductometric titration, using a Mettler Toledo pH meter with a conductivity probe. The fibers of the CMC modified electrospun cellulose scaffold and controls were carefully separated with tweezers in DI water. Thereafter, the fibers were sonicated to aid in dispersion. The electrospun cellulose dispersion was pretreated with 100 mL of HCl 0.1N for 1 h at 300 rpm and room temperature followed Katz procedure.³⁸ The pretreated fibers were rinsed several times with DI water. The dispersion of the electrospun cellulose fibers (approximately 0.22 g of dry weight) for titration was prepared by the addition of 0.001 mol of NaCl, 5 mL of HCl 0.1N and DI water to a total volume of 350 mL. The conductometric titration was carried out under nitrogen atmosphere. A volume of 0.25 mL of NaOH 0.1N was added every 5 min before and after the conductivity plateau zone was reached. In the conductivity plateau zone, 0.1 mL of NaOH was added in 5 min intervals. Normally, titration was stopped at approximately pH 10.5.

Biomimetic Coating of Ca-P Crystals. Simulated body fluid (SBF) solution was prepared according to Cüneyt Tas procedure³⁴ and stored at 5 °C for no longer than a month during its use. The chemical composition of SBF solution is listed in Table 1. A comparison between ion concentration in SBF solution used in this study and the human plasma is shown in Table 2. The SBF solution was prepared by adding

the chemicals sequentially until complete dissolution of each salt, in the order showed in Table 1. Fifteen mL of HCl 0.1 N solution was added before the addition of calcium chloride, to avoid calcium chloride precipitation as suggested within the procedure. Finally, the temperature was increased to 37 °C and the pH adjusted at 7.4 by the addition of (CH₂OH)₃CNH₂ (0.5 g/L) and HCl (25 mL/L) to mimic physiological conditions. Regenerated cellulose scaffolds (45 min and 24 h) without surface modification, CMC treated scaffolds at the different conditions, and reference scaffolds at the conditions of the second CMC treatment (pH 8, 80 °C for 2 h) were treated with SBF solution. The SBF treatment consisted of the static exposure of 1 cm by 1 cm sections of the cellulose scaffolds to 15 mL of SBF solution at 37 °C. The SBF solution was refreshed every day during 1 week. After the SBF treatment was completed, the samples were rinsed in distilled water several times and lyophilized for further characterization.

Scaffold Characterization. Surface morphological and microstructural features of the samples were investigated by scanning electron microscopy, LEO (Zeiss) 1550 and Neoscope from Nikon Instruments. The analysis was carried out for freeze-dried samples coated in gold–palladium with thickness of 35 to 40 Å. Fourier-Transform infrared (FTIR) spectroscopic analysis, 8700 Nicolet Thermo Electron, in transmission mode, was used in the wavenumber range of 4000–500 cm⁻¹ to measure the relative degree of regeneration into cellulose of the electrospun scaffolds. Experimental FTIR spectra of solid samples were obtained by preparing KBr pellets with ratio of 1:99 (1 mg to 99 mg) sample-to-KBr, and scanned at a resolution of 4 cm⁻¹ and averaged over 64 scans. The surface chemical composition of the scaffold nanofibers was quantified with a scanning photoelectron spectrometer (XPS) Microprobe PHI Quantera SXM with a highly focused monochromatic X-ray beam. A rectangular area of 1 mm by 0.1 mm was scanned on the surface of the samples. In order to analyze the crystalline structure of the electrospun scaffolds and determine the identity of the produced crystals, X-ray powder diffraction (XRD, Bruker D8 Discover)

was performed from 2θ values of 10 to 60° for regenerated cellulose samples and samples treated with SBF.

RESULTS

Electrospun Cellulose Acetate (CA) Scaffold. Several electrospinning preliminary screening experiments were performed with aim to investigate the effect of polymer concentration, solvent selection, voltage and distance between needle and collector. In most cases, fibers with bead-enriched morphology were obtained. Similar findings were reported elsewhere.^{29–32} The conditions selected as described in the experimental section, based on 13% (w/w) polymer solution in acetone/DMAc 1:2, resulted in a bead-free nonwoven scaffold with polydisperse fiber size. The diameter of the CA fibers was estimated to be in the range of 200 nm to 1.5 μm (see Figure 1), in agreement with other authors.^{10,29–31} The thickness of the dried scaffold was 0.0254 cm. The surface texture of a single fiber can be observed in the SEM micrograph (Figure 1).

Regeneration of the Electrospun Scaffolds. Fibers of electrospun CA were regenerated to cellulose via alkali saponification with 0.05 M NaOH ethanol solution at room temperature using previously described procedures.^{2,10,29–31} In order to distinguish the degree of regeneration and create a CA-cellulose blend of different composition, the time of hydrolysis was varied for further studies of modification. The regeneration process was monitored by analyzing the scaffold composition using FTIR spectroscopy and XPS. FTIR spectra as a function of deacetylation time show characteristic changes in cellulose acetate when exposed to alkali (Figure 2). The spectrum of CA scaffold (0 min exposure to NaOH) has absorption peaks for carbonyl stretching at 1750 cm⁻¹ (ν C=O), alkoxy stretch of the ester at 1235 cm⁻¹ (ν C—O—C), and methyl bending at 1370 cm⁻¹ (δ C—CH₃), for groups of the acetate substituent.^{10,29–31} The acetal linkages of the cellulose backbone can be observed around 1160 cm⁻¹ and the broad hydroxyl group absorption at approximate 3400 cm⁻¹.³¹ The intensity of absorption peaks at 1750, 1370, and 1235 cm⁻¹ related to the acetyl group content decreased as the time of regeneration increased. It can be observed the broadening of the hydroxyl absorption with the increase in time of regeneration; this change illustrates the substitution of acetyl groups with hydroxyl groups. After 24 h of treatment, the carbonyl peak had completely disappeared (Figure 2), which supported the claim that nearly complete regeneration into cellulose of the electrospun fibers had been achieved at that point. Of particular

Table 2. Ion Concentrations of SBF Solutions and Human Plasma³⁴

ion	human blood (mM)	present work (mM)
Na ⁺	142.0	142.0
Cl ⁻	103.0	125.0
HCO ³⁻	27.0	27.0
K ⁺	5.0	5.0
Mg ²⁺	1.5	1.5
Ca ²⁺	2.5	2.5
HPO ²⁻	1.0	1.0
SO ²⁻	0.5	0.5

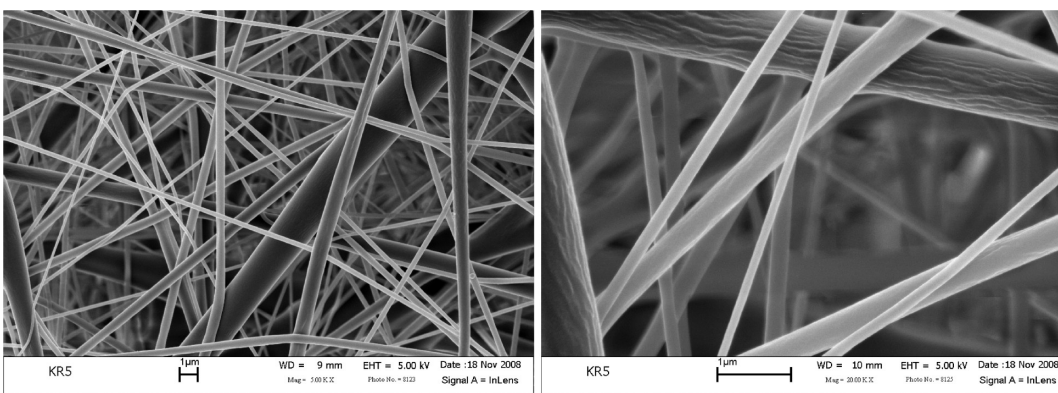


Figure 1. SEM images of CA scaffold.

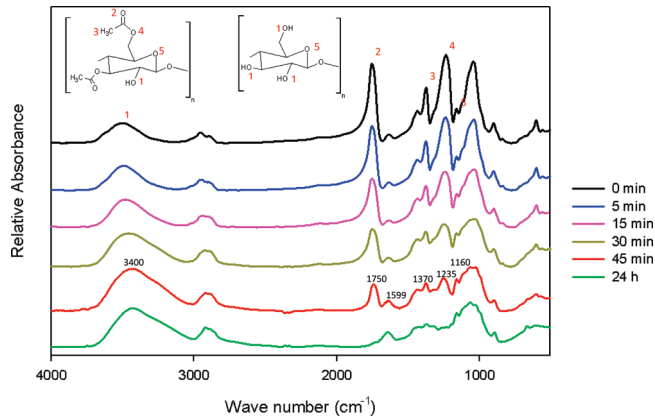


Figure 2. FTIR spectra of CA and regenerated cellulose scaffolds as a function of exposure time in NaOH/ethanol.

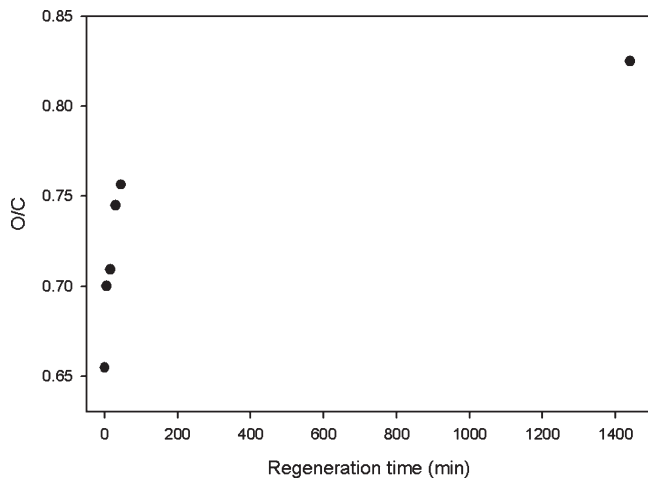


Figure 3. Atomic O/C surface ratio of CA and regenerated cellulose scaffolds as a function of exposure time in NaOH/ethanol.

interest in this study was the presence of carboxylate (COO^-) groups, due to its capacity to induce $\text{Ca}-\text{P}$ crystal formation, indicated by the asymmetric stretching vibration at 1599 cm^{-1} for all samples.³⁹ Furthermore, an increase in intensity of the carboxylate group was detected as result of the regeneration process, as observed in other studies.^{10,29} The carboxylate group formation may be attributed to cellulose scission and aerobic oxidation, a well-known process in alkaline hydrolysis of cellulose.⁴⁰

The time for complete regeneration differed with a previous study by Liu and Hsieh as they reported near complete deacetylation for electrospun CA for equal DS after 60 min of treatment with NaOH/ethanol at the same concentration.³⁰ However, the authors reported that there are still acetyl groups as the degree of substitution was found to be 0.15. Furthermore other studies have reported longer regeneration times at higher alkali concentrations were required.^{10,29} The inconsistency of regeneration times demonstrates the difficulty in describing the kinetics of heterogeneous deacetylation for electrospun cellulose acetate where different electrospinning parameters impact fiber diameter.

Surface chemistry of cellulose regeneration was analyzed by XPS. The XPS results (see Figure 3) showed an increase in atomic concentration of oxygen relative to atomic carbon with the increase in regeneration time. This behavior supported the

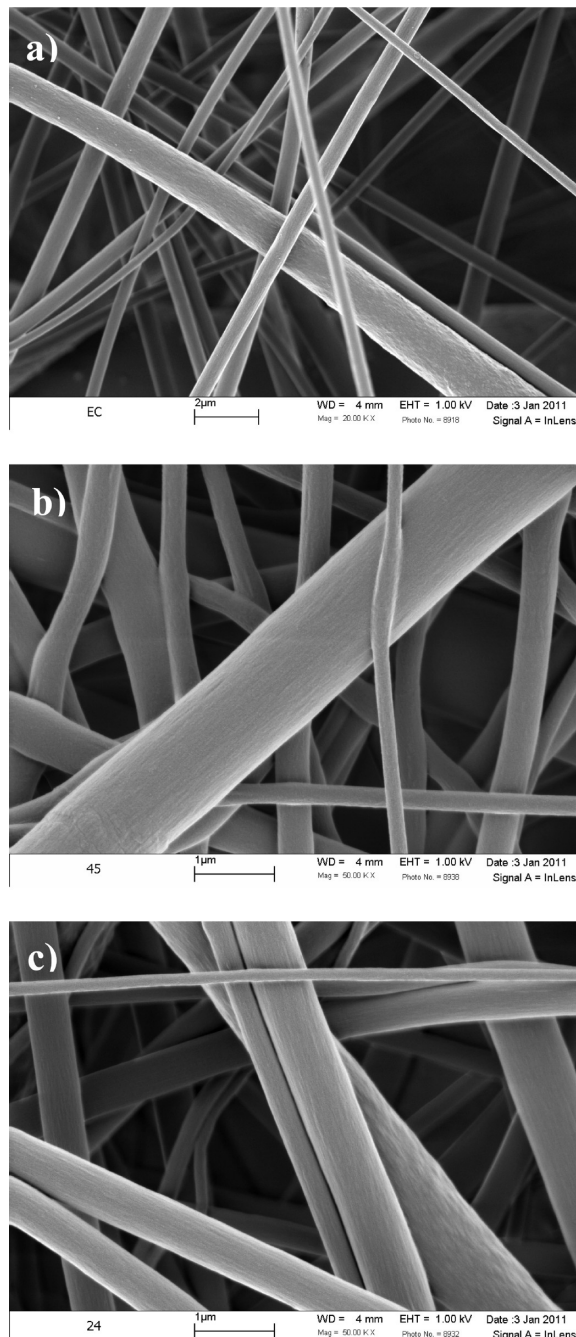


Figure 4. SEM images of (a) CA and regenerated cellulose at (b) 45 min and (c) 24 h of treatment in NaOH/ethanol.

substitution of acetyl by hydroxyl groups due to the saponification reaction on the fibers surface. For 45 min and lower time regenerated samples, the fibrous mat still retains some acetyl groups within the first 10 nm of the fiber surface. Either the outermost surface is not fully saponified or the layer near the maximum probe depth is not. It was observed that at 24 h of hydrolysis the theoretical O/C ratio value for cellulose, according to⁴¹ and,⁴² had been reached. This value indicates that a complete surface regeneration of CA fibers into cellulose was accomplished at 24 h of deacetylation treatment. Surface and bulk regeneration of the CA nonwoven scaffold had shown a similar trend as demonstrated by FTIR and XPS analysis.

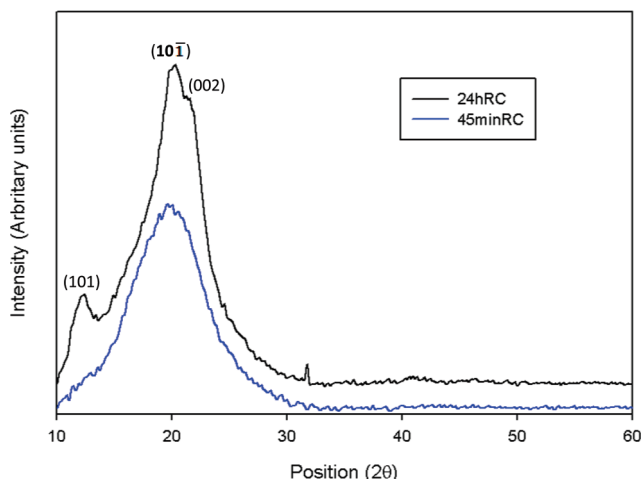


Figure 5. XRD diffractograms of cellulose scaffolds regenerated for 45 min and 24 h treatment in NaOH/ethanol.

Fiber Morphology. The nonwoven mesh structure of CA was well preserved during the conversion into cellulose, as can be observed in the SEM images (Figure 4). There was no change in morphology of the fibers due to deacetylation treatment after 45 min and 24 h. Furthermore, minimal swelling occurred in agreement with other studies for alkali-ethanol system.^{30,31} This result showed that cellulose-based scaffolds can be produced and designed from CA in order to take advantage of its expanded processability window compared to cellulose, including properties such as solubility, T_g , and T_m which can be influenced by either the degree of acetylation or the addition of a plasticizing agent. X-ray analysis of the electrospun mats after regeneration (45 min and 24 hrs) shows changes in its morphological structure (Figure 5). The fiber sample after 24 h regeneration has sharp peaks associated with the crystal structure of cellulose II located at angles of 12°, 20°, and 22°, similar to what is shown by Fink and co-workers.⁴³ The cellulose II diffraction pattern was expected since the regeneration process was carried out by NaOH treatment. The 45 min regenerated cellulose sample only presented one broad signal at 20° and that peak was wider than that showed by the 24 h RC sample. The electrospinning process rapidly removes solvent preventing preferred packing of cellulose acetate chains. Control of the crystalline structure is expected to impact the *in vivo* stability and mechanical performance of the scaffold, providing a wider range of properties that can be controlled to impact scaffold performance by regenerating cellulose to varying degrees.

CMC Adsorption and Calcium Ion Content. Toluidine blue staining method was sensitive to detect the thin layer of CMC adsorption on the fiber surfaces. As observed in Figure 6, the cationic dye stained the CMC treated cellulose fibers indicating surface modification. Conductometric titration was carried out (see Table 3) to further quantify the carboxyl content introduced by the CMC adsorption process. This technique revealed an initial concentration of COOH groups in the control regenerated cellulose sample, as observed by FTIR (Figure 2). The CMC modified samples registered a 2.3 fold increase for procedure 1 and 2.6 fold increase for procedure 2 in the carboxyl content.

Since the Ca–P crystal formation is influenced by the initial attachment of Ca ions to the cellulose fiber surface, XPS was performed to compare the efficiency of CMC treated versus nonmodified samples to retain Ca ions after CaCl_2 exposure. The

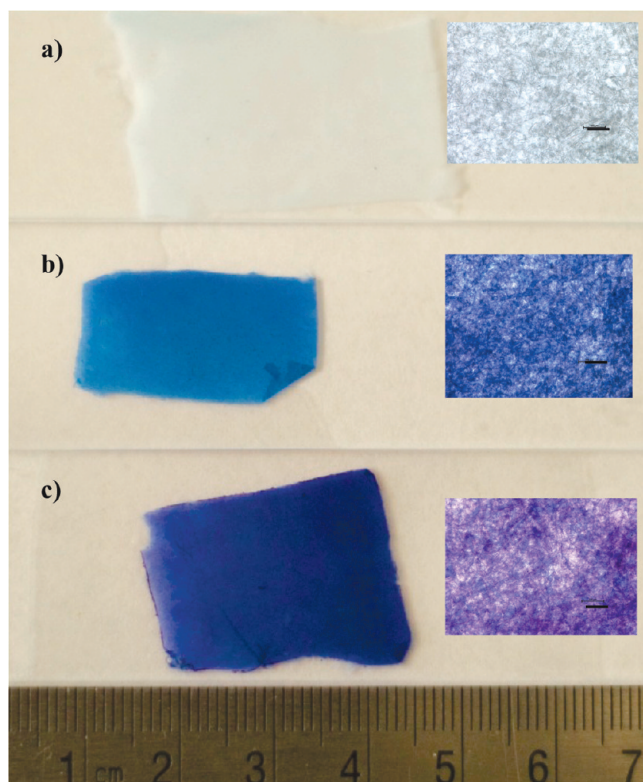


Figure 6. Scaffolds treated with the cationic dye toluidine blue to qualitatively analyze CMC treatment (a) 24 h regenerated cellulose, (b) 24 regenerated cellulose treated with CMC for 24 h, room temperature, pH 7, and (c) 24 h regenerated cellulose treated with CMC for 2 h at 80 °C and pH 8. Magnified surfaces are shown with the scale bar indicating 100 μm .

Table 3. Carboxyl Content on Regenerated and CMC-Modified Electrospun Cellulose Quantified by Conductometric Titration

sample	COOH concentration (mmol/g of sample)
control	
24 h control (no CMC)	0.104
procedure 1	
24 h CMC modified	0.240
control treated at elevated temperature	
24 h treated at conditions of procedure 2 (no CMC)	0.111
procedure 2	
24 h CMC modified	0.270

results are shown in Table 4. The atomic surface concentration of calcium for all the samples was less than 1%. The scaffolds for 45 min and 24 h of regeneration without CMC treatment presented absence or lower concentrations of calcium. The regenerated cellulose controls treated at the conditions of procedure 2, without CMC, had a 4-fold increase in the calcium content for the 24 h regenerated sample. Additionally, in the presence of CMC, procedure 2 was more efficient than procedure 1 in calcium attachment, as there was twice the calcium amount for the 24 h regenerated samples and 10 times the calcium amount

for the 45 min regenerated samples. These results suggest that Ca ion attachment to regenerated cellulose fibers surface can be enhanced either by heat treatment or carboxyl group presence. It is also evident that 24 h regenerated samples is more efficient in the calcium loading than the 45 min regenerated samples.

Biomimetic Coating of Ca-P Crystals. Regenerated scaffolds without CMC were exposed to SBF solution to determine if

Table 4. Atomic Surface Calcium Concentration on Regenerated and CMC Modified Electrospun Cellulose Soaked in CaCl_2 Solution and Rinsed with Water

sample	C1s	O1s	O/C	Ca2p
control				
45 min RC control	56.16	43.84	0.78	0
24 h RC control	55.29	44.71	0.81	0.01
procedure 1				
45 min RC CMC modified	56.35	43.63	0.77	0.02
24 h RC CMC modified	55.54	44.29	0.80	0.18
control treated at elevated temperature				
45 min RC treated at conditions of procedure 2 (no CMC)	56.14	43.84	0.78	0.02
24 h RC treated at conditions of procedure 2 (no CMC)	55.73	44.23	0.79	0.04
procedure 2				
45 min RC CMC modified	57.45	42.36	0.74	0.20
24 h RC CMC modified	55.91	43.71	0.78	0.39

the fibers could be used to nucleate Ca-P crystallization. The samples shown in Figure 7 indicate that regenerated cellulose with only a room temperature soak in CaCl_2 solution prior to exposure to SBF (Figure 7A,B), show marginal activity in forming crystals. This result suggested that regenerated electrospun cellulose can induce crystal formation under SBF treatment, albeit weakly (Figure 7A,B). It is seen in these images that random areas along the fiber surfaces show mineralized clusters, a micrometer or larger in diameter, for both regeneration times. The formation of minerals on the fibers may arise from the carboxylate groups formed during the slight oxidative degradation during alkaline saponification (Figure 2) and quantified by conductometric titration (Table 3).

The samples that were exposed to elevated temperature in a slightly alkaline solution in the presence of CaCl_2 , reveal additional mineralization (Figure 7C&7D). The additional mineralization may arise from greater loading of the Ca^{2+} ions on the fiber surface as seen in Table 3. While the time of regeneration for samples in Figure 7A and Figure 7B does not appear to influence the mineralization process, the degree of regeneration for the higher temperature soak does influence the mineralization process. Qualitative analysis of the images consistently shows increased mineralization for the 24 h-regenerated fibers, as the fibers are more decorated with mineralized clusters. Note that exposure of the 45 min scaffold to alkali at 80 °C causes additional saponification, but FTIR data shows that it retains acetyl groups (not shown). In summary, it appears that cellulose scaffolds treated with CaCl_2 at room temperature are weakly

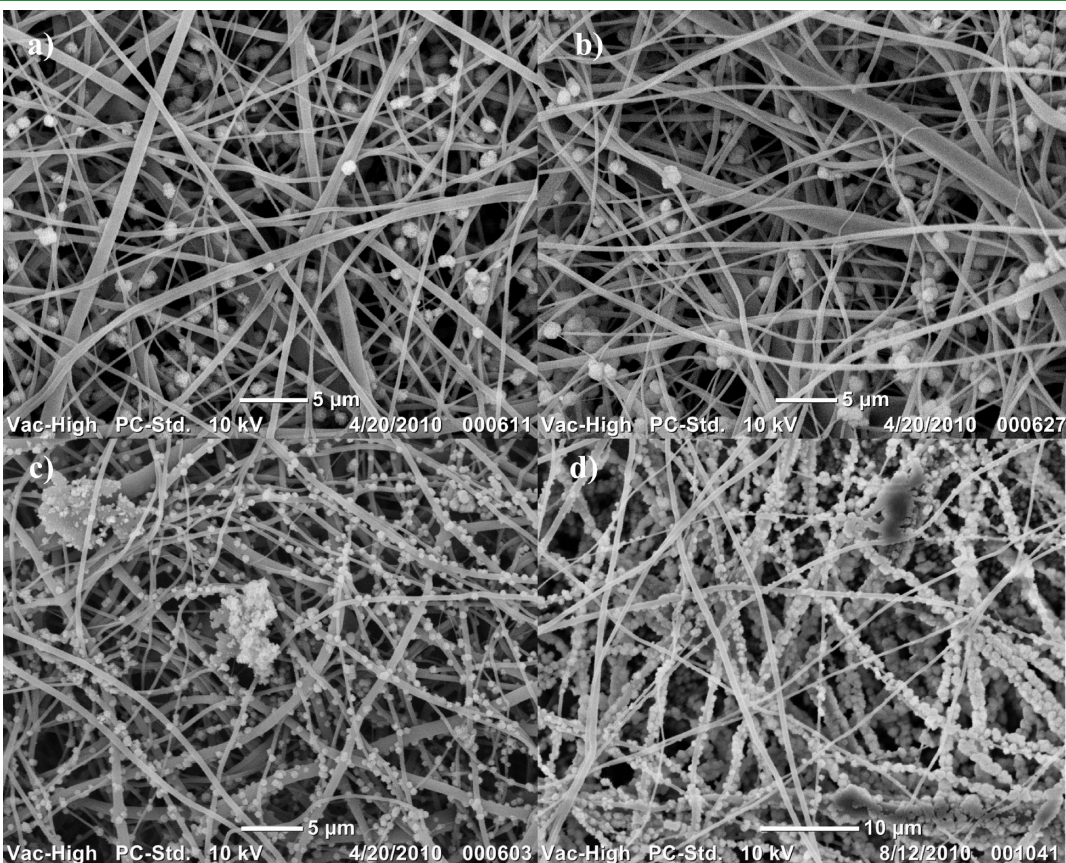


Figure 7. SEM of mineralized scaffolds without CMC pretreatment (A) 45 min regeneration time, (B) 24 h regeneration time, (C) 45 min regeneration time combined with treatment at 80 °C, pH 8 for 2 h, and (D) same as C but with 24 h regeneration time.

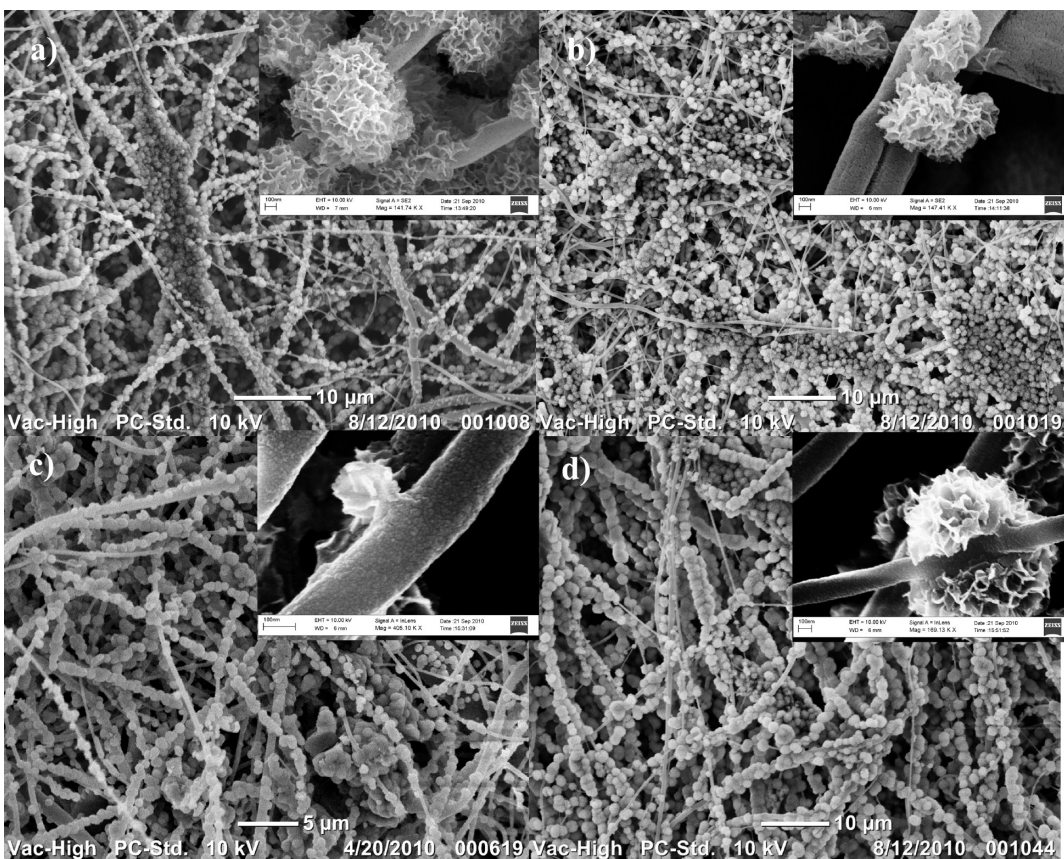


Figure 8. SEM of mineralized scaffold with CMC treatment (A) 45 min RC and (B) 24 h RC treated with procedure 1, (C) 45 min RC, and (D) 24 h RC treated with procedure 2.

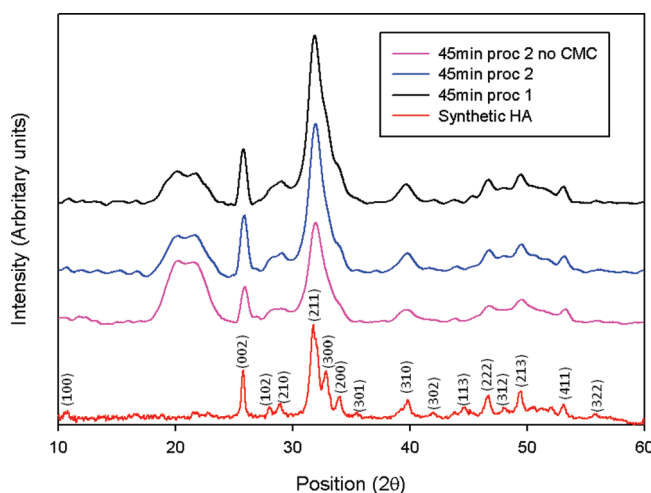


Figure 9. Mineralized samples after 45 min regeneration exposed to simulated body fluid for 1 week.

bioactive and this bioactivity, shown through mineralization, is enhanced after CaCl_2 treatment at elevated temperature.

Cellulose fibers treated with CMC exhibits crystal mineralization (Figure 8). Both CMC treatment methods with either procedure 1 (adsorption at room temperature for 24 h) or procedure 2 (adsorption at elevated temperature and pH for 2 h) appear effective in inducing mineralization. In one of the inset images (Figure 8D), the mineral structure appears as a

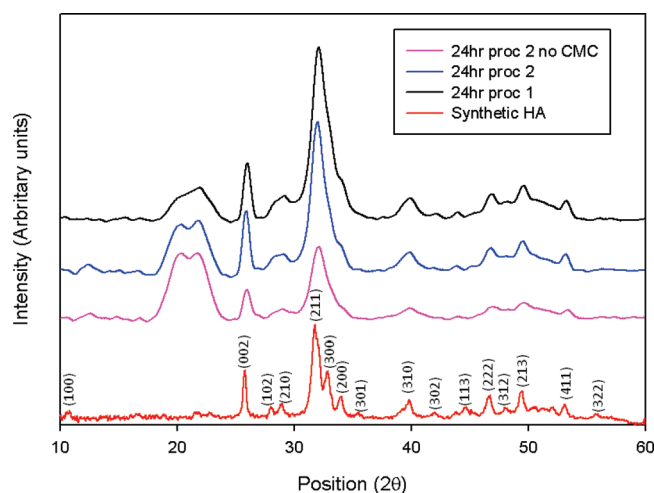


Figure 10. Mineralized samples after 24 h regeneration exposed to simulated body fluid for 1 week.

"blossom" on the fiber surface, while other images show the mineralization process proceeding further, continuing to wrap around the fiber providing a pearl-on-string type of arrangement.

X-ray diffraction patterns were recorded to investigate the chemical structure of the mineralized scaffolds (Figures 9 and 10). Synthetic HA (Sigma-Aldrich) was analyzed by XRD and used as a HA reference. The synthetic HA was indexed using a powder diffraction files (see Figures 9 and 10). XRD peaks

observed at 2θ equal to 25.8, 31.8, 32.9, 34.0, 39.7, 46.6, 49.4, and 53.1 correspond to HA as highlighted by the reference spectrum (Figures 9 and 10).^{25,44} The HA XRD peaks were observed for all the samples treated with SBF. This result clearly indicates that Ca–P crystals or deficient HA was formed on the electrospun cellulose fibers due to the SBF treatment. Moreover, limited differences were found within the diffractograms between the two mineralization procedures (including the control sample of procedure 2). This data suggests a wide range of possibilities to achieve a mineralized scaffold with slightly altered structures from a single polymer material (cellulose acetate). The above results suggest a future study of the mechanical properties of the fibers due to regeneration extent in order to determine the critical performance criteria along with durability and degradation of the cellulose-based scaffolds. Evaluation of the bioactivity due to mineralization *in vivo* needs to be performed to further complement these *in vitro* studies.

■ DISCUSSION

Biomimetic mineralization was shown to occur *in vitro* on cellulose substrates that were surface modified via noncovalent methods. For *in vivo* biomimetic mineralization, intermolecular interactions and ion solvation impacts crystal nucleation and ion transport to the surface impacts crystal growth. In the cellulose system, scaffolds with trapped calcium ions had created the nucleation sites that interact with phosphate ions during the simulated body fluid (SBF) treatment to produce Ca–P crystals. Evident of this mechanism was the differences in crystal growth for the control samples (no CMC) from procedure 1 and procedure 2 (Figure 7). Calcium contents prior to SBF treatment were greater for the samples that were treated at elevated temperature (Table 4). In fact, calcium content for the control treated at conditions of procedure 2 with 24 h regeneration was similar to the calcium content for the CMC treated sample from procedure 1 with 45 min regeneration. Comparing Figure 7d to Figure 8a, it is difficult to distinguish differences in crystal growth, further pointing to the presence of the calcium ions on the surface controlling crystal growth.

The XRD data shows that most of the peaks related to hydroxyapatite are very broad (Figure 9 and 10). This result is similar to the diffraction pattern of extracted bone mineral from zebrafish fin rays that contain smaller sized and a lower degree of mineralization, relative to synthetic hydroxyapatite.⁴⁶ Hence, mineralized cellulosic scaffolds share similar features to the diffractograms from *in vivo* produced bone mineral. Another difference found in the XRD data for the scaffolds relative to the synthetic hydroxyapatite (Figures 9 and 10) is the broadening of the peak at 29° with increased intensity. Powder diffraction of amorphous Ca/P revealed a broad scattering peak located between 25 and 35° .^{46,48} On the basis of this data, it is suggested that amorphous Ca/P is also present within the SBF treated scaffold. This finding is significant because mineralization is indicated to occur for many systems with clusters of amorphous minerals that transform into crystalline apatite.^{46,47} It was suggested that anionic polymers help stabilize these calcium and phosphate packages.⁴⁶ Very low concentrations (nM to μ M) of solubilized polymeric additives affect the mineralization process.⁴⁵ In other words, these polymer-mediated clusters serve as Ca/P reservoirs for integration into platelets within the collagenous network. For successful tissue integration, surfaces that contain mixed Ca/P clusters should enhance mineralization

in vivo, whereas synthetically produced hydroxyapatite may not promote tissue growth in the same way.

Finally, we noticed a qualitative change in mechanical properties after mineralization as the scaffold became rigid. Nature uses the mineralization process to enhance the stiffness of biomaterials, as mechanical performance scales with mineral content. As cellulose is the most abundant polymer on the planet, conversion of cellulose into hard materials at ambient conditions provides a path to modify cellulose on the surface enabling adoption in new applications. The above data strongly suggests that biomimetic mineralization of electrospun cellulose from cellulose acetate has attributes to make it regarded as a novel biomaterial.

■ CONCLUSION

CA regeneration can be carried out by NaOH ethanol solution with minimal degradation of the cellulose while retaining the original fiber structure of the electrospun mat. The morphology of the partially regenerated cellulose revealed only a broad diffraction peak for the scaffold material. The fully regenerated cellulose showed characteristic cellulose II diffraction pattern. A qualitative dye probe indicated that the fibers were readily modified with anionic groups through the physically adsorption of carboxymethylcellulose (CMC) in the presence of CaCl_2 . Conductometric titration measurements confirmed the increase of carboxylic groups due to the CMC adsorption process. HA-like minerals were formed on the electrospun cellulose scaffolds for all the CaCl_2 treated samples. The samples were able to nucleate crystal growth by the process of pretreating the scaffolds by heating in aqueous alkali in the presence of CaCl_2 . Biomimetic coating of Ca–P crystals on electrospun fibers was significantly enhanced by the carboxyl groups added by the charging process with CMC. CMC adsorption on the scaffolds created equal opportunity for mineralization on either the 45 min or 24 h regenerated scaffold. Since the surface is the only area of the material in contact with physiological environment, this finding implicates the process of controlling the CMC adsorption and calcium loading to the substrate material for the creation of mineralized scaffolds. This enhanced Ca–P mineralization on cellulose scaffolds can be accomplished by either increasing the negative charge (COO^-) or aqueous heating treatment in the presence of Ca ions. Mineralization within a SBF solution indicated that cellulose scaffolds could be made into a bioactive substrate that can be further studied for bone tissue engineering applications.

■ AUTHOR INFORMATION

Corresponding Author

*E-mail: srenneck@vt.edu.

■ ACKNOWLEDGMENT

This project was supported by the USDA NIFA AFRI Grant 2010-65504-20429, USDA CSREES, Special Research Grant 2008-34489-19377, Institute of Critical Technology and Applied Science of Virginia Tech, and the Wallenberg Wood Science Center of Sweden. The authors acknowledge the Sustainable Engineered Materials Institute of Virginia Tech for providing access to equipment used in this research. For assistance with the XRD and microscopy additional expertise was provided by Rick Caudill and Dr. Audrey Zink-Sharp of the Wood Science and

Forest Products Department. In addition, the authors wish to thank to Dr. Niven Monsegue of Materials Science and Engineering Department at Virginia Tech for support in XRD characterization, Dr. Anke Sanz-Velasco of Department of Microtechnology and Nanoscience, Chalmers University of Technology, and Stephen McCartney from Nanoscale Characterization and Fabrication Laboratory at Virginia Tech for additional SEM characterization. Finally, the authors would like to thank Dr. Zhiyuan Lin, Qingqing Li, and Wei Zhang for their assistance in carrying out conductometric titration measurements.

■ REFERENCES

- (1) Lannutti, J.; Reneker, D.; Ma, T.; Tomasko, D.; Farson, D. *Mater. Sci. Eng., C* **2007**, *27*, 504–509.
- (2) Entcheva, E.; Bien, H.; Yin, L.; Chung, C. Y.; Farrell, M.; Kostov, Y. *Biomaterials* **2004**, *25*, 5753–5762.
- (3) Pajulo, O.; Viljanto, J.; Hurme, T.; Saukko, P.; Lönnberg, B.; Lönnqvist, K. *J. Biomed. Mater. Res.* **1996**, *32*, 439–446.
- (4) Mårtson, M.; Viljanto, J.; Hurme, T.; Laippala, P.; Saukko, P. *Biomaterials* **1999**, *20*, 1989–1995.
- (5) Klemm, D.; Schumann, D.; Udhardt, U.; Marsch, S. *Prog. Polym. Sci.* **2001**, *26*, 1561–1603.
- (6) Müller, F. A.; Müller, L.; Hofmann, I.; Greil, P.; Wenzel, M. M.; Staudenmaier, R. *Biomaterials* **2006**, *27*, 3955–3963.
- (7) Miyamoto, T.; Takahashi, S.; Ito, H.; Inagaki, H.; Noishiki, Y. *J. Biomed. Mater. Res.* **1989**, *23*, 125–133.
- (8) Hofmann, I.; Müller, L.; Greil, P.; Müller, F. *Surf. Coat. Technol.* **2006**, *20*, 2392–2398.
- (9) Dan Dimitrijevich, S.; Tatarko, M.; Gracy, R. W.; Linsky, C. B.; Olsen, C. *Carbohydr. Res.* **1990**, *195*, 247–256.
- (10) Ma, Z.; Ramakrishna, S. *J. Membr. Sci.* **2008**, *319*, 23–28.
- (11) Laurence, S.; Bareille, R.; Baquey, C.; Fricain, J. C. *J. Biomed. Mater. Res., Part A* **2005**, *73A*, 422–429.
- (12) Fundueanu, G.; Constantin, M.; Esposito, E.; Cortesi, R.; Nastruzzi, C.; Menegatti, E. *Biomaterials* **2005**, *26*, 4337–4347.
- (13) Fricain, J. C.; Granja, P. L.; Barbosa, M. A.; de Jeso, B.; Barthe, N.; Baquey, C. *Biomaterials* **2002**, *23*, 971–980.
- (14) Zimmermann, K. A.; LeBlanc, J. M.; Sheets, K. T.; Fox, R. W.; Gatenholm, P. *Mater. Sci. Eng., C* **2011**, *31*, 43–49.
- (15) Ponader, S.; Brandt, H.; Vairaktaris, E.; von Wilmowsky, C.; Nkenke, E.; Schlegel, K. A.; Neukam, F. W.; Holst, S.; Müller, F. A.; Greil, P. *Colloids Surf., B* **2008**, *64*, 275–283.
- (16) Bäckdahl, H.; Helenius, G.; Bodin, A.; Nannmark, U.; Johansson, B. R.; Risberg, B.; Gatenholm, P. *Biomaterials* **2006**, *27*, 2141–2149.
- (17) Andrade, F. K.; Costa, R.; Domingues, L.; Soares, R.; Gama, M. *Acta Biomater.* **2010**, *6*, 4034–4041.
- (18) Kino, Y.; Sawa, M.; Kasai, S.; Mito, M. *J. Surg. Res.* **1998**, *79*, 71–76.
- (19) Gerlach, J.; Stoll, P.; Schnoy, N.; Schauwecker, H. *J. Hepatol.* **1988**, *7*, S135–S135.
- (20) Maneerung, T.; Tokura, S.; Rujiravanit, R. *Carbohydr. Polym.* **2008**, *72*, 43–51.
- (21) Czaja, W.; Krystynowicz, A.; Bielecki, S.; Brown, R. M. *Biomaterials* **2006**, *27*, 145–151.
- (22) McCullen, S. D.; Hanson, A. D.; Lucia, L. A.; Loba, E. G. *Nanoscience and Technology of Renewable Biomaterials*; John Wiley & Sons: Chichester, U.K., 2009; pp 293–314.
- (23) Bartouilh de Taillac, L.; Porté-Durrieu, M. C.; Labrugère, C.; Bareille, R.; Amédée, J.; Baquey, C. *Compos. Sci. Technol.* **2004**, *64*, 827–837.
- (24) Svensson, A.; Nicklasson, E.; Harrah, T.; Panilaitis, B.; Kaplan, D. L.; Brittberg, M.; Gatenholm, P. *Biomaterials* **2005**, *26*, 419–431.
- (25) Grande, C. J.; Torres, F. G.; Gomez, C. M.; Carmen Bañó, M. *Acta Biomater.* **2009**, *5*, 1605–1615.
- (26) Wan, Y. Z.; Huang, Y.; Yuan, C. D.; Raman, S.; Zhu, Y.; Jiang, H. J.; He, F.; Gao, C. *Mater. Sci. Eng., C* **2007**, *27*, 855–864.
- (27) Rhee, S. H.; Tanaka, J. *J. Mater. Sci.: Mater. Med.* **2000**, *11*, 449–452.
- (28) Frey, M. W. *Polym. Rev.* **2008**, *48*, 378–391.
- (29) Ma, Z.; Kotaki, M.; Ramakrishna, S. *J. Membr. Sci.* **2005**, *265*, 115–123.
- (30) Han, S. O.; Youk, J. H.; Min, K. D.; Kang, Y. O.; Park, W. H. *Mater. Lett.* **2008**, *62*, 759–762.
- (31) Liu, H.; Hsieh, Y. L. *J. Polym. Sci., Part B: Polym. Phys.* **2002**, *40*, 2119–2129.
- (32) Tungprapa, S.; Puangparn, T.; Weerasombut, M.; Jangchud, I.; Fakum, P.; Semongkhon, S.; Meechaisue, C.; Supaphol, P. *Cellulose* **2007**, *14*, 563–575.
- (33) Kim, C. W.; Kim, D. S.; Kang, S. Y.; Marquez, M.; Joo, Y. L. *Polymer* **2006**, *47*, 5097–5107.
- (34) Cüneyt Tas, A. *Biomaterials* **2000**, *21*, 1429–1438.
- (35) Laine, J.; Lindström, T.; Nordmark, G. G.; Risinger, G. *Nord. Pulp Pap. Res. J.* **2000**, *15*, 520–526.
- (36) Fras-Zemlič, L.; Stenius, P.; Laine, J.; Stana-Kleinschek, K. *Cellulose* **2006**, *13*, 655–663.
- (37) Isogai, T.; Saito, T.; Isogai, A. *Biomacromolecules* **2010**, *11*, 1593–1599.
- (38) Katz, S. *Svensk Papperstidn.* **1984**, *6*, 48–53.
- (39) Chen, S.; Kimura, K. *Langmuir* **1999**, *15*, 1075–1082.
- (40) Knill, C. J.; Kennedy, J. F. *Carbohydr. Polym.* **2003**, *51*, 281–300.
- (41) Fras, L.; Johansson, L. S.; Stenius, P.; Laine, J.; Stana-Kleinschek, K.; Ribitsch, V. *Colloids Surf., A* **2005**, *260*, 101–108.
- (42) Johansson, L. S.; Campbell, J. M.; Koljonen, K.; Stenius, P. *Appl. Surf. Sci.* **1999**, *144*–*145*, 92–95.
- (43) Fink, H. P.; Hofmann, D.; Philipp, B. *Cellulose* **1995**, *2*, 51–70.
- (44) Hutchens, S. A.; Benson, R. S.; Evans, B. R.; O'Neill, H. M.; Rawn, C. J. *Biomaterials* **2006**, *27*, 4661–4670.
- (45) Elhadj, S.; De Yoreo, J. J.; Hoyer, J. R.; Dove, P. M. *Proc. Natl. Acad. Sci.* **2006**, *103*, 19237–19242.
- (46) Mahamida, J.; Aichmayer, B.; Shimonic, E.; Ziblata, R.; Lib, C.; Siegelb, S.; Parisd, O.; Fratzlb, P.; Weinera, S.; Addadia, L. *Proc. Natl. Acad. Sci.* **2010**, *107*, 6316–6321.
- (47) Weiner, S.; Sagi, I.; Addadi, I. *Science* **2005**, *309*, 1027–1028.
- (48) Glimcher, M. *J. Rev. Mineral. Geochem.* **2006**, *64*, 223–282.